2 October 1981, Volume 214, Number 4516 SCIENCE

A Major Helium-3 Source at 15°S on the East Pacific Rise

John E. Lupton and Harmon Craig

Summary. An extensive plume of water enriched with helium-3 has been discovered in the deep Pacific Ocean at latitude 15°S on the East Pacific Rise. In the core of the plume, at a depth of 2500 meters over the ridge crest, the helium-3/helium-4 ratio is 50 percent higher than the ratio in atmospheric helium, indicating a strong injection of mantle or primordial helium at the spreading center axis through local hydrothermal systems. The helium-3 plume is completely absent east of the rise, but it can be traced over 2000 kilometers to the west above a newly observed physical feature: a density discontinuity here called the "ridge-crest front." The injected plume provides a unique deep-sea tracer with an asymmetric distribution which shows that the deep circulation across the rise is from east to west. The striking intensity and lateral extent of this helium-3 anomaly, compared to observations at known oceanic hydrothermal sites, suggest that the largest hydrothermal fields in the ocean are yet to be discovered and that they will be found near 15°S on the East Pacific Rise.

One of the major inputs into the terrestrial helium budget is the flux of primordial helium from the mantle into the oceans and, in turn, into the atmosphere and interplanetary space. The existence of this flux was established by helium isotope measurements in deep Pacific Ocean water (*1, 2*), in oceanic basalts (*3*), and in discharges from submarine hydrothermal vents (*4, 5*). The distinct isotopic ratio of this mantle helium ($^3He/^4He \simeq 10^{-5}$) makes it possible to detect small amounts of this component in the presence of atmospheric helium ($^3He/^4He \simeq 10^{-6}$) or helium produced by radioactive decay ($^3He/^4He \simeq 10^{-7}$) (*6*). Helium-3 is not a useful atmospheric tracer because its residence time in the atmosphere is of the order of 10^6 years, much longer than the mixing time of the atmosphere itself. However, in the deep oceans the ^3He residence time is about 4000 years, comparable to oceanic mixing times, and the primordial helium injected at sea-floor spreading centers produces measurable oceanic $^3He/^4He$ variations which are extremely useful for deep circulation studies. We have reviewed the current knowledge of helium isotope geochemistry elsewhere (*7*); in this article we describe a dramatic application of helium injection in the deep sea to oceanic circulation and mixing studies.

As one might expect, the ^3He enrichment observed in the deep oceans varies with the scale of tectonic activity: while significant ^3He enrichments have been found in only a few places in the Atlantic (*8*), the East Pacific Rise axis, with its very high spreading rates, is a source of high ^3He concentrations throughout the deep Pacific (*2*). Although the Pacific is ideal for ^3He tracer studies, the distribution of the injection sites along the rise must be fairly well known before variations in the $^3He/^4He$ ratio can be used to define deep circulation patterns. Unfortunately, the Geosecs expedition (*9*), which has furnished most of the data concerning the general ^3He distribution in the Pacific, did not provide coverage of the principal ^3He input regions on the East Pacific Rise. In this article we present a series of $^3He/^4He$ profiles collected over the East Pacific Rise during Scripps Institution of Oceanography expedition South Tow, and show how injection of helium at this latitude provides a remarkable tracer for deep-ocean circulation. This work, an eastward extension of the Geosecs net, represents one of the first steps in the important process of mapping specific ^3He injection sites in the eastern Pacific.

Experimental Methods

Seawater samples were collected in Niskin hydrographic bottles and transferred without exposure to air into 40-milliliter copper-tubing containers for storage. The dissolved gases, including helium, neon, argon, and nitrogen, were later extracted and purified in a high vacuum line. Ratios of ^3He to ^4He were determined with a dedicated 25-centimeter-radius, double-collecting mass spectrometer (*3, 8*). The precision for the $^3He/^4He$ measurements, based on the reproducibility of air samples used as standards, is standard deviation = 0.7 percent. Splits of these samples were also analyzed for absolute helium and neon concentrations on a separate mass spectrometer, using isotope dilution. These absolute concentrations, which are accurate to ~ 0.5 percent, will be discussed in detail elsewhere (*10*).

The authors were, respectively, assistant research physicist and professor of geochemistry and oceanography, Scripps Institution of Oceanography, University of California at San Diego, La Jolla 92093, when this work was done. John E. Lupton is now an associate research oceanographer at the Marine Science Institute, University of California at Santa Barbara 93106.

0036-8075/81/1002-0013$01.00/0

East Pacific Rise Section at 15°S

The data reported here consist of seven profiles collected during leg 8 of expedition South Tow (*11*). As shown in Fig. 1, these stations form an east-west section over the East Pacific Rise extending from 90° to 134°W longitude at latitude approximately 15°S. Analytical data from South Tow include shipboard measurements of temperature, salinity, oxygen, and silicate and shore-based determinations of ^{3}He, ^{4}He, other dissolved gases, and ^{226}Ra; the hydrography and ^{226}Ra results have been discussed by Chung (*12*).

The South Tow ^{3}He/^{4}He results are listed in Table 1 and plotted against depth in Fig. 2 in units of $\delta(^3\text{He})$, the percentage deviation of the ^{3}He/^{4}He ratio from the ratio in air (*13*). The most striking feature of these data is immediately apparent: the $\delta(^3\text{He})$ profiles show a pronounced east-west asymmetry due to ^{3}He injection at the East Pacific Rise crest at this latitude. This strong east-west gradient over the crest is not found in any other property measured in these samples (including temperature, silicate, and dissolved neon, argon, nitrogen, and radon). The three profiles to the east of the ridge crest (stations 1, 2, and 3) are similar to others reported (*2, 5*) in the eastern Pacific: $\delta(^3\text{He})$ increases smoothly with depth to a broad maximum of 28 to 30 percent between depths of 2000 and 3000 meters. This 30 percent excess in the ^{3}He/^{4}He ratio observed in eastern Pacific deep water is due to widespread ^{3}He injection associated with the tectonic activity of the East Pacific Rise system (*2*). However, at 112°W longitude on the rise crest, there is clear evidence for local ^{3}He injection: a sharp ^{3}He plume appears at 2500 m in the profile at station 4. This sharp maximum in $\delta(^3\text{He})$, which is absent in the eastern basin profiles, is seen in all the profiles to the west, including that at station 7, more than 2000 kilometers from the spreading center axis.

With the exception of the high ^{3}He enrichments found within the restricted geometry of the Guaymas Basin in the Gulf of California (*14*), the maximum value of $\delta(^3\text{He})$ = 50 percent observed at South Tow station 4 is the highest ^{3}He/^{4}He value reported for an open-ocean sample. The magnitude and lateral extent of this ^{3}He anomaly are even more impressive when compared with those at sites where a ^{3}He input has been verified. For example, at the Galápagos Rift and at 21°N on the East Pacific Rise, where direct hydrothermal injection of ^{3}He has been observed at submarine vents (*4, 5*), the ^{3}He enrichments in the water column are not as large as those at 15°S. But more significantly, the integrated ^{3}He excess relative to ambient water at 15°S is much greater than at the other sites. The ^{3}He distribution at 15°S therefore implies a very strong flux from the East Pacific Rise at this latitude, an observation which is consistent with the very high spreading rates (~ 15 cm/year) estimated for this section of the Pacific-Nazca plate junction (*15*).

The east-west asymmetry in ^{3}He at 15°S is strikingly portrayed in Fig. 3, in which $\delta(^3\text{He})$ is contoured in section view across the ridge. Figure 3 also shows that the apparent depth of ^{3}He injection (~ 2500 m) is some 400 m shallower than the average depth of the ridge crest at this latitude. Surveys of the ridge bathymetry in this vicinity have shown that an axial ridge or a series of central peaks rises 100 to 400 m above the flank of the ridge crest (*15, 16*), and thus the discrepancy between the depth of the ^{3}He plume center and the average bot-

Table 1. Helium isotope measurements from South Tow expedition.

Depth (m)	Potential temperature (°C)	Salinity (per mil)	$\delta(^3\text{He})$ (%)
Station 1 (15°59′S, 89°57′W; depth, 4496 m)			
3	21.15	35.793	−0.6*
395	8.33	34.596	5.0
702	5.59	34.508	10.3
1251	3.47	34.560	23.2
1585	2.72	34.602	25.7
1870	2.33	34.622	28.8
2160	2.00	34.635	29.1
2748	1.61	—	29.4
3590	1.51	34.683	25.6
3883	1.48	34.686	25.8
4177	1.44	34.687	25.9
Station 2 (14°00′S, 103°00′W; depth, 4189 m)			
4	23.25	35.729	−2.0*
697	6.03	34.530	10.3
994	4.40	34.528	17.3
1205	3.71	34.559	19.1
1239	3.55	34.555	19.7
1480	2.98	34.582	24.4
1869	2.29	34.627	26.8
2668	1.59	34.674	26.7
2966	1.56	34.677	26.7
3262	1.53	34.675	28.2
3567	1.51	34.677	26.7
3870	1.50	34.677	25.9
4186	1.49	34.678	26.9
Station 3 (15°51′S, 108°02′W; depth, 3645 m)			
1	23.55	35.876	−1.8*
685	5.88	34.504	11.0
979	4.25	34.524	16.4
1226	3.48	34.554	19.7
1491	2.83	34.593	24.8
1773	2.41	34.620	25.7
1951	2.09	34.638	29.3
2154	1.88	34.650	29.1
2365	1.72	34.661	29.4
2571	1.63	34.667	29.4
2783	1.60	34.669	28.0
2991	1.57	34.671	26.4
3206	1.56	34.672	27.3
3417	1.54	34.672	26.1
3628	1.54	34.672	25.5
Station 4 (13°36′S, 112°19′W; depth, 3041 m)			
936	4.68	34.523	13.4
1174	3.70	34.557	19.5
1425	2.98	34.589	24.0
1578	2.67	34.603	26.3
1738	2.42	34.614	26.7
1892	2.16	34.628	29.9
2210	1.75	34.657	37.6
2371	1.70	34.664	43.2
2529	1.65	34.670	50.5
Station 4 (13°36′S, 112°19′W; depth 3041 m)			
2693	1.64	34.672	47.1
3014	1.62	34.670	37.6
Station 5 (12°00′S, 119°43′W; depth, 3660 m)			
3	25.78	35.494	−1.9*
391	8.91	34.645	3.7
694	6.04	34.534	8.6
994	4.39	34.529	14.9
1235	3.47	34.563	20.8
1466	2.92	34.593	23.6
1681	2.48	34.615	25.9
1900	2.16	34.631	28.0
2114	1.91	34.648	32.2
2334	1.72	34.664	37.9
2549	1.63	34.671	39.3
2770	1.57	34.675	34.3
2986	1.47	34.677	29.0
3209	1.35	34.681	24.5
3426	1.26	34.688	21.8
3646	1.22	34.684	20.6
Station 6 (12°37′S, 126°00′W; depth, 3774 m)			
5	25.75	35.788	−2.4*
392	9.01	34.643	3.3
975	4.47	34.521	15.0
1217	3.57	34.551	19.9
1287	3.34	34.561	21.5
1529	2.82	34.588	23.9
2018	1.95	34.640	32.2
2268	1.73	34.657	38.2
2513	1.64	34.667	39.3
2763	1.58	34.667	34.6
3009	1.48	34.671	28.7
3262	1.38	34.675	24.9
3513	1.30	—	26.8
3764	1.26	34.682	21.4
Station 7 (14°00′S, 134°04′W; depth 4430 m)			
4	26.47	36.050	−2.2*
391	10.39	34.590	0.5
691	5.74	34.498	11.6
988	4.20	34.522	16.2
1230	3.34	34.555	19.8
1553	2.58	34.595	23.9
1835	2.11	34.629	28.4
2122	1.81	34.651	31.8
2406	1.66	34.661	33.0
2695	1.55	34.667	30.9
2977	1.43	34.675	27.3
3267	1.35	34.677	23.8
3553	1.27	34.679	20.8
3847	1.23	34.682	20.3
4132	1.18	34.690	20.1
4420	1.16	34.684	19.3

*Surface $\delta(^3\text{He})$ values have been corrected for tritium decay during sample storage (*30*). The expected value for surface seawater in equilibrium with air is $\delta(^3\text{He})$ = −1.4 percent because of the difference in isotope solubilities (*31*).

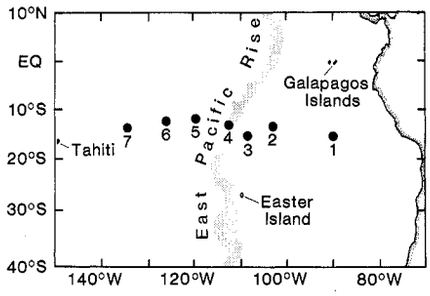

Fig. 1. Location of hydrographic stations on South Tow expedition.

tom topography may be due to ^{3}He injection at the crest of this central ridge. However, since the ^{3}He input almost certainly occurs through hydrothermal vents, the height of the ^{3}He maximum above the bottom is likely to be caused by the rising of hot vent water as buoyant filaments or plumes. These filaments are analogous to smokestack plumes, in which the hot buoyant effluent rises and mixes with the ambient medium until density equilibrium is achieved and lateral spreading occurs. As shown in Fig. 3, we have not sampled the rising filaments of vent water directly, but rather have detected the core of ^{3}He-rich water produced by the vent water after it has reached density equilibrium. At 21°N on the East Pacific Rise, a similar but less pronounced ^{3}He-rich layer is found ~ 200 m above the hydrothermal vents at this site (*5, 17*). Thus the 400-m depth difference and the higher $\delta(^3\text{He})$ values observed at 15°S indicate that this is a much more powerful source than the 21°N area.

Summing up the phenomena pictured in Fig. 3, we see a ^{3}He "plume" at a depth of 2500 m, injected by hydrothermal activity, which then spreads horizontally and uniquely to the west, where it is traceable for thousands of kilometers. In magnitude, scale, and striking asymmetry, this plume is one of the most remarkable features of the deep ocean, resembling a volcanic cloud injected into a steady east wind.

One possible mechanism which could produce such a skewed spatial distribution is a much stronger rate of vertical mixing east of the East Pacific Rise, which erases the plume by rapid mixing of the water column. This hypothesis can be tested by examining a measure of the vertical mixing rate: the buoyancy gradient (or the square of the Vaisala frequency) $[(g/\rho)\ (\partial\rho_{POT}/\partial z)]$, which has been shown to be inversely proportional to the vertical eddy diffusion coefficient in certain regimes (*18*). We calculated this parameter for the South Tow stations by using the discrete bottle data (Table 1). Although east of the ridge the very deep water below 3000 m is less stable than the equivalent water to the west (due to its lower temperature gradient), in the critical 2200- to 3000-m depth interval which spans the zone of ^{3}He injection there is no difference in stability east and west of the rise. Thus it is highly unlikely that a difference in vertical mixing rates can explain the observed ^{3}He asymmetry, and this conclusion is supported by the lack of evidence for rapid vertical mixing to the east in the profiles of any other properties. We now show that the ^{3}He plume axis (defined by the ^{3}He maximum in vertical section) lies just above a physical feature of the water column clearly associated with westward advection across the East Pacific Rise.

Ridge-Crest Front: A Mid-Depth Density Discontinuity

In Fig. 4 we show the potential density profiles along the 15°S section. Immediately apparent is a discontinuity in the density profiles west of the ridge, occurring at depths of 2700 to 2850 m. This discontinuity, which lies just 300 m below each ^{3}He maximum, in fact follows the 45.84 per mil isopycnal surface at

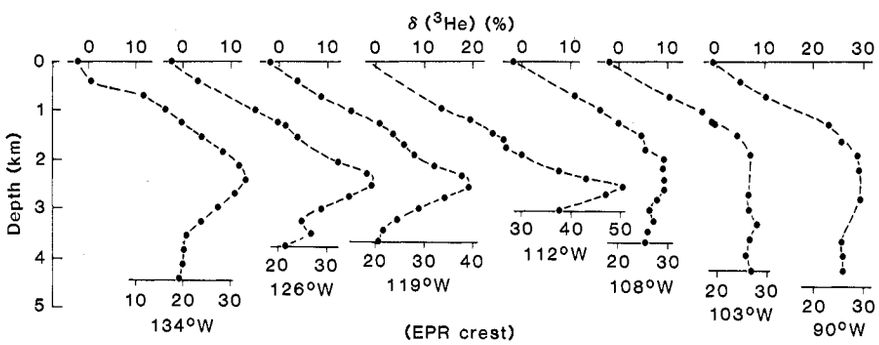

Fig. 2. Profiles of $\delta(^3\text{He})$ at latitude ~15°S across the East Pacific Rise (*EPR*).

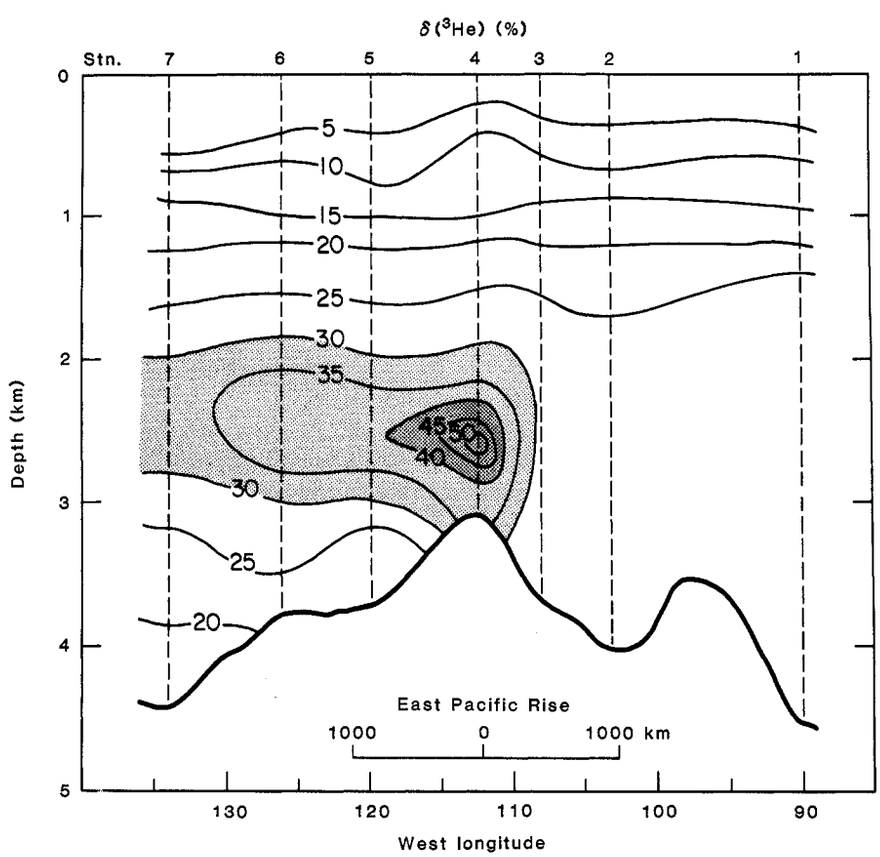

Fig. 3. Contours of $\delta(^3\text{He})$ in section view over the East Pacific Rise at 15°S. Note that the center of the ^{3}He plume is ~ 400 m above the ridge crest.

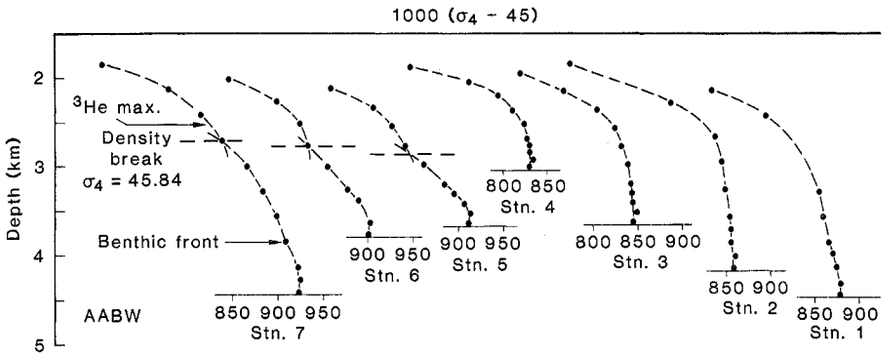

Fig. 4. Density profiles along the 15°S East Pacific Rise section. The σ_4 denotes the deviation from unity of the potential density at the 400-bar (~ 4000 m depth) pressure surface, in parts per thousand.

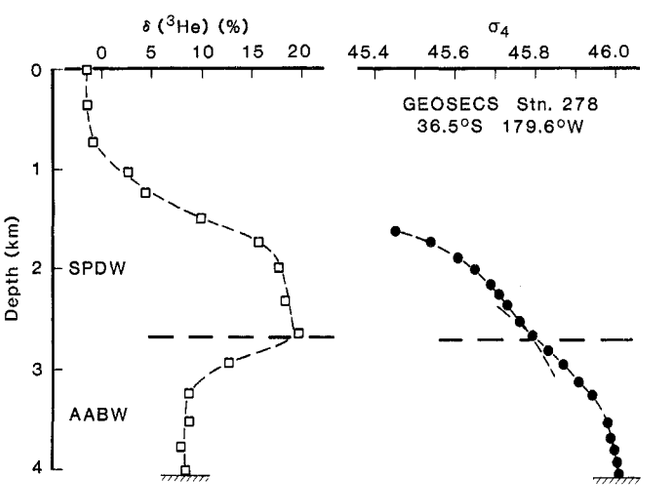

Fig. 5. Plots of $\delta(^3He)$ and σ_4 (see legend to Fig. 4) at Geosecs station 278 in the southwest Pacific. The dashed line is the benthic front density discontinuity (*19*), which separates South Pacific Deep Water (*SPDW*) from Antarctic Bottom Water (*AABW*).

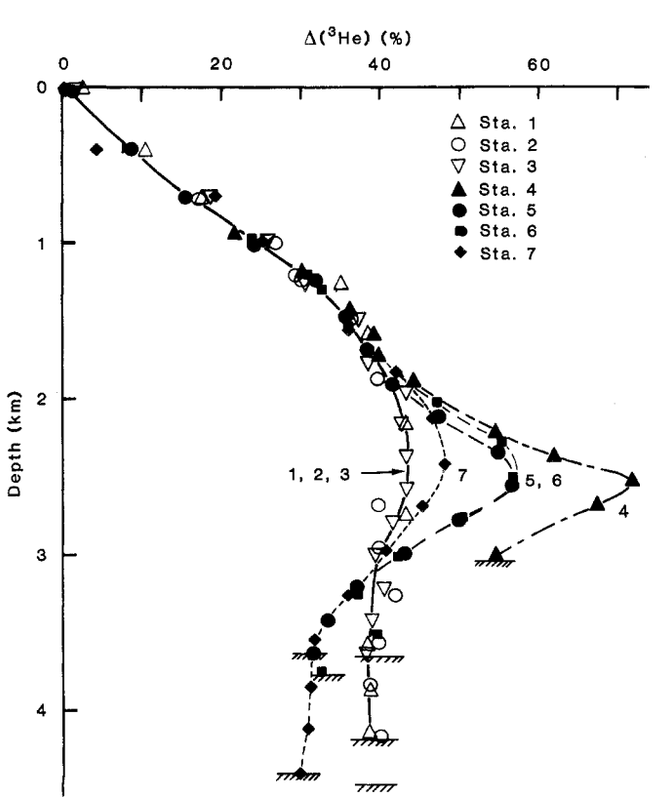

Fig. 6. Plots of $\Delta(^3He)$, the ^{3}He concentration anomaly, as a function of depth at the seven South Tow stations (*24*). Note that the profiles at stations 5 and 6 are essentially identical.

stations 5, 6, and 7, clearly marking a boundary between two water masses with different density profiles. This phenomenon was observed previously in the deep Pacific farther west and south, where the "benthic front" separates the South Pacific Deep Water mass from the underlying Antarctic Bottom Water (*19*).

Figure 5 shows an example of the benthic front, at Geosecs station 278 in the southwest Pacific, near the region of the initial discovery of the ^{3}He mid-depth maximum in the oceans (*1*). Here the ^{3}He maximum is also associated with a potential density discontinuity on almost the same isopycnal (45.84 per mil) surface and, as with other extrema on this surface, the ^{3}He extremum is an "induced maximum," simply due to the juxtaposition of high-^{3}He water over the much lower ^{3}He Antarctic Bottom Water (*20*). The benthic front is here essentially a depth of "no motion" between southward-moving deep water and the underlying Antarctic Bottom Water flowing northward from the Circumpolar Current (*19*). In Fig. 4, in the westernmost profile at station 7, the benthic front (which deepens north and west of Geosecs 278) is just seen in the second density discontinuity at 3900 m; at station 6 the ridge is too shallow and the front is gone.

Astonishingly, in this region the deep Pacific Ocean contains two density discontinuities and three discrete layers below a depth of 2 km. The upper discontinuity—by analogy, the "ridge-crest front"—is not observed east of the rise (Fig. 4); thus the flow above the ridge crest has a strong east-to-west component—the deepwater "east wind"—while beneath the front west of the rise the flow is in a different direction.

The classic Stommel-Arons deepwater geostrophic circulation model (*21*) is characterized by southeasterly flow throughout a homogeneous water mass in this region, but such models necessarily neglect the effects of strong topographic barriers and cannot be expected to reproduce the horizontal flow patterns in a structured water column adjacent to a large ridge like the East Pacific Rise. Indeed, one important application of these ridge-crest helium plumes will be the clear picture of local flow patterns they provide for comparison with complicated deepwater circulation models which include effects of sea-floor geometry and topography.

One effect of the East Pacific Rise as a topographic barrier is seen as differences in the deepwater potential temperature and $^3He/^4He$ profiles to the east and west of the rise crest. Potential temperatures in the eastern basin at depths of 3000 to

4000 m average ~ 0.30°C higher than west of the rise axis, a feature which has been reported previously (*22, 23*). This temperature offset is due to the intervening topography. The deep water in the basins to the east of the rise must be supplied by input of relatively shallow warm water through a series of sills and passages. This east-west difference in the bottom-water composition is also evident in the $\delta(^3He)$ values: at depths below 3500 m $\delta(^3He)$ averages 26 percent to the east of the rise and only 20 percent to the west (Fig. 3). The lower temperature and $\delta(^3He)$ of the bottom water on the western flank of the rise are due to the effect of Pacific Bottom Water of circumpolar origin (*22*), which cannot cross the rise crest. This western flank water [potential temperature, $\theta = 1.2°C$, $\delta(^3He) = 20$ percent] could be synthesized by mixing equal parts of Pacific Bottom Water [$\theta = 0.8°C$, $\delta(^3He) = 8$ to 10 percent] and Pacific Deep Water [$\theta = 1.65°C$, $\delta(^3He) = 30$ to 35 percent]. Thus the large vertical gradients in $\delta(^3He)$ are accentuated at depths between 2500 and 4000 m at stations 5, 6, and 7 because the ^3He-rich deep water (1500 to 3500 m) mixes with the underlying bottom water (> 3500 m), which is relatively depleted in ^3He.

Helium-3 Concentrations in Deep Water

For quantitative studies of circulation and mixing, the absolute concentration of each isotope is required (that is, ratios do not "diffuse"). In Fig. 6, we show profiles of the ^3He "concentration anomaly," $\Delta(^3He)$, which is the percentage deviation of the ^3He concentration from solubility equilibrium with atmospheric helium (*24*). Plotting the concentration data in this way shows two very striking features of the profiles. First, from the surface to ~ 1800 m, all profiles in this region are essentially identical. Antarctic Intermediate Water produces a marked salinity minimum as an advective feature at 700 to 900 m, but the effect on other properties is hardly noticeable. Second, the almost identical profiles at stations 5 and 6, separated in space by some 700 km, is very puzzling. In an equivalent distance along the core of the plume from station 4 to station 5 the ^3He anomaly decreases from 72 to 57 percent, and from station 6 to station 7 from 57 to 48 percent. Clearly, there is a much more complicated structure here (perhaps a gyre) than can be seen in two dimensions, and more mapping of this complicated feature will be necessary to understand the circulation pattern in detail.

Helium-3/Helium-4 Ratio of the Injected Helium

One way to estimate the isotopic ratio of helium injected into deep water at ridge crests is to use the relation between the concentration or solubility anomaly $\Delta(^3He)$ and the ratio anomaly $\delta(^3He)$, since these must be related by the $^3He/^4He$ ratios of atmospheric and mantle helium. In Fig. 7 we show this relation for the South Tow samples; surprisingly, the data form a well-defined linear array over the entire range of $\Delta(^3He) = 0$ to 70 percent. Theoretically, this relation is not expected to be linear, since it involves a three-component mixture of "solubility-equilibrium" helium, air helium, and mantle helium (*2*). In fact, however, the $\Delta(^3He)$ versus $\delta(^3He)$ relation can be calculated a priori, given the measured neon and helium concentrations and known solubilities, as a function of the $^3He/^4He$ ratio in the injected mantle helium (*25*). Three such calculated curves are shown in Fig. 7 for various $^3He/^4He$ ratios in the injected mantle component; comparison with the measured data indicates that the $^3He/^4He$ ratio (R) of the injected mantle helium is between 7.5 and 9.0 times the atmospheric ratio (R_{ATM}). The Δ-δ relation is therefore predictable and happens to be linear for $R \simeq 8\ R_{ATM}$ (*25*). The best-fit value, $R \simeq 8.0\ R_{ATM}$, is the ratio observed in hydrothermal fluids from submarine vents (*4*) and, most recently, in both fluids and fresh glass from the 21°N field of 350°C hydrothermal vents (*5, 26*).

The relation in Fig. 7 is important for the following reasons: It is possible to determine from $\Delta(^3He)$ versus $\delta(^3He)$ relations measured in different regions whether a single isotopically uniform type of helium is injected everywhere in the oceans and, if not, to obtain an idea of the relative source strengths. For example, if isotopically different helium is injected from bottom sediments in a basin in significant quantities, then a different $\Delta(^3He)$ versus $\delta(^3He)$ relation would be observed. However, the data presented here represent some of the highest helium concentrations observed in the oceans, and since the enrichments are smaller throughout most of the oceans, the importance of high-precision isotope dilution measurements of the absolute concentrations of both helium and neon is apparent.

Other Plume Components

Welhan and Craig (*27*) observed a large flux of abiogenic methane accompanying ^3He in the 21°N hydrothermal vents; the estimated flux from the entire ridge system (based on the $CH_4/^3He$ ratio and the oceanic ^3He flux) is sufficient

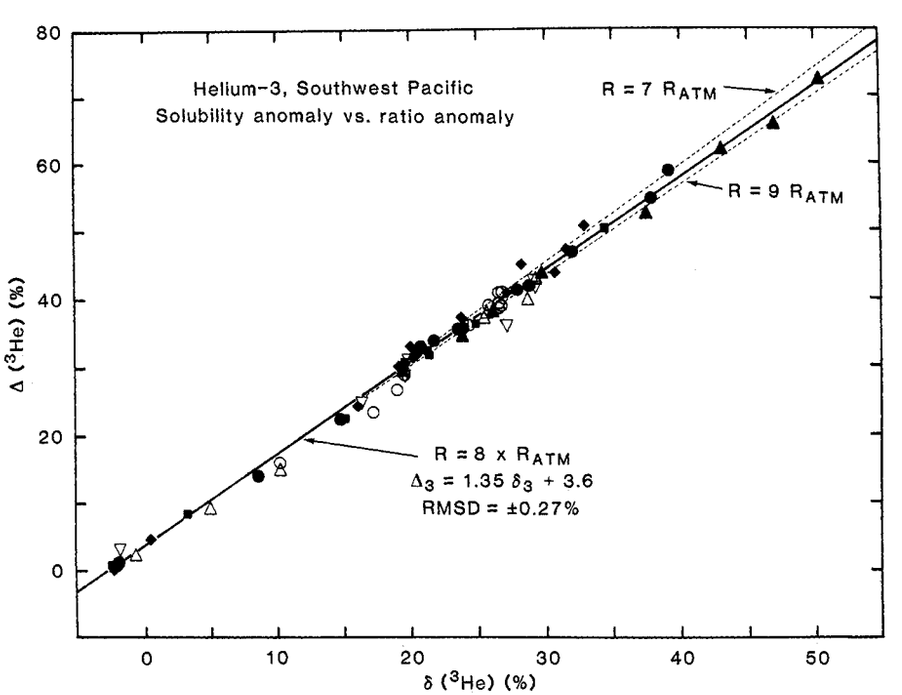

Fig. 7. The ^3He concentration anomaly, $\Delta(^3He)$, versus the $^3He/^4He$ ratio anomaly, $\delta(^3He)$, for the South Tow data at 15°S across the East Pacific Rise. The station symbols are the same as in Fig. 6. The solid line is the calculated $\Delta(^3He)$ versus $\delta(^3He)$ relation for mixtures of atmospheric helium and mantle-injected helium with $^3He/^4He$ about 8 times the atmospheric ratio, R_{ATM}. Dashed lines are the calculated curves for $R = 7$ and 9 times R_{ATM} (*25*). *RMSD* is the root-mean-square deviation.

to replace all the oceanic methane in about 30 years. Thus methane must be nonconservative in the deep sea, and if the methane consumption rate can be approximately established, the $CH_4/^3He$ ratio along the plume axis will provide a "speedometer" for the abyssal circulation in this region.

Manganese is highly enriched in hydrothermal emissions (*5, 28*); it is scavenged rapidly from the water column by sinking particulate matter on a time scale of 50 to 100 years (*29*). The scavenging of manganese from the 15°S East Pacific Rise plume will produce a "manganese plume shadow" on the underlying sediment on the western flanks of the rise. The exact shape of this shadow will be affected by the north-south component of abyssal flow and by the relative rates of sinking of particulates and horizontal advection. The shadow will thus provide additional information on the circulation, and the expression of the manganese shadow deeper in the sediments may provide fascinating information about paleocirculation as well as paleoinjection sites along the East Pacific Rise.

Conclusions

This remarkable sequence of eastern Pacific ^3He profiles clearly demonstrates the uniqueness of ^3He as a deep ocean tracer. The $\delta(^3He) = 50$ percent value at the East Pacific Rise crest (13°S, 112°W) is the highest "open-ocean" ^3He enrichment reported to date; it occurs as a sharp maximum at 2500 m superimposed on the general eastern Pacific background value of $\delta(^3He) = 30$ percent and points to a strong ^3He source on the East Pacific Rise near 15°S. The effects of this ^3He injection are observed more than 2000 km west of the spreading center, but they are completely absent only 450 km to the east. The asymmetric ^3He distribution, together with the mid-depth density discontinuity or ridge-crest front associated with the ^3He plume west of the rise, shows that westward advection of deep water occurs across the rise at 15°S, a pattern which is not predictable from the classic geostrophic models developed for flat ocean basins.

The relation between $^3He/^4He$ isotope ratios and ^3He concentration shows that at 15°S on the East Pacific Rise injected mantle helium has an $^3He/^4He$ ratio approximately eight times the atmospheric ratio, as also observed at the hydrothermal vent sites at 21°N on the East Pacific Rise and at the Galápagos spreading center. The similarity of these ratios is further evidence for a very uniform and characteristic helium isotope ratio in helium injected at world-ocean ridge crests (*7*).

This striking emission of ^3He along ridge crests, accompanied by strong fluxes of methane, manganese, and other trace gases and metals, provides a plume filled with unique tracers for studies or oceanic circulation, particulate fluxes, and other phenomena. Perhaps most important, the tremendous extent and source strength of the ^3He plume at 15°S are strong indications that the largest hydrothermal fields in the ocean are yet to be found and that they are present in this region of 15° to 20°S on the East Pacific Rise.

References and Notes

1. W. B. Clarke, M. A. Beg, H. Craig, *Earth Plant. Sci. Lett.* **6**, 213 (1969); *J. Geophys. Res.* **76**, 7676 (1970).
2. H. Craig, W. B. Clarke, M. A. Beg, *Earth Planet. Sci. Lett.* **26**, 125 (1975).
3. J. E. Lupton and H. Craig, *ibid.*, p. 122; H. Craig and J. E. Lupton, *ibid.* **31**, 369 (1976).
4. J. E. Lupton, R. F. Weiss, H. Craig, *Nature (London)* **262**, 244 (1977); *ibid.* **267**, 602 (1977); W. J. Jenkins, J. M. Edmond, J. B. Corliss, *ibid.* **272**, 156 (1978).
5. J. E. Lupton, G. P. Klinkhammer, W. R. Normark, R. Haymon, K. Macdonald, R. F. Weiss, H. Craig, *Earth Planet. Sci. Lett.* **50**, 115 (1980).
6. P. Morrison and J. Pine, *Ann. N.Y. Acad. Sci.* **62**, 69 (1955).
7. H. Craig and J. E. Lupton, in *The Sea*, vol. 7, *The Oceanic Lithosphere*, C. Emiliani, Ed. (Wiley, New York, in press).
8. W. J. Jenkins, M. A. Beg, W. B. Clarke, P. J. Wangersky, H. Craig, *Earth Planet. Sci. Lett.* **16**, 122 (1972); W. J. Jenkins and W. B. Clarke, *Deep-Sea Res.* **23**, 481 (1976); J. E. Lupton, *Earth Planet. Sci Lett.* **32**, 371 (1976).
9. H. Craig and K. K. Turekian, *Earth Planet. Sci. Lett.* **49**, 263 (1980).
10. J. E. Lupton, in preparation.
11. The data for all the stations discussed here are on file at the Physical and Chemical Oceanographic Data Facility of the Scripps Insitution of Oceanography.
12. Y. Chung, *Earth Planet. Sci. Lett.* **49**, 319 (1980).
13. The ratio anomaly is defined as $\delta(^3He) = (R/R_{ATM} - 1) \times 100$, where $R = {}^3He/^4He$ and $R_{ATM} = 1.40 \times 10^{-6}$.
14. J. E. Lupton, *J. Geophys. Res.* **84**, 7446 (1979).
15. D. K. Rea, *Mar. Geophys. Res.* **2**, 291 (1976); *Earth Planet. Sci. Lett.* **34**, 78 (1977).
16. P. Lonsdale, *Mar. Geophys. Res.* **3**, 295 (1977).
17. RISE Project Group, *Science* **207**, 1421 (1980).
18. J. L. Sarmiento, H. W. Feely, W. S. Moore, A. E. Bainbridge, W. S. Broecker, *Earth Planet. Sci. Lett.* **32**, 357 (1976). In the equation, g is the gravitational constant, 980.665 cm/sec^2, ρ is density, and ρ_{POT} is potential density.
19. H. Craig, Y. Chung, M. Fiadeiro, *ibid.* **16**, 50 (1972).
20. Ironically, it was this induced maximum which was responsible for the hypothesis that the excess ^3He represented primordial helium emitted at ridge crests and spreading throughout the oceans. Although this is, in fact, true, the maximum in the South Pacific is due to the induced effect of the front.
21. H. Stommel and A. B. Arons, *Deep-Sea Res.* **6**, 217 (1960).
22. P. Lonsdale, *J. Geophys. Res.* **81**, 1163 (1976).
23. A. W. Mantyla, *J. Mar. Res.* **33**, 341 (1975).
24. The concentration anomaly Δ_3 is related to the ratio anomaly δ_3 by $\alpha\ \Delta_3 = \delta_3 + \Delta_4 + 10^{-2}\delta_3\Delta_4 - \epsilon$ [H. Craig and W. B. Clarke, *Earth Planet. Sci. Lett.* **9**, 45 (1970)]. Here $\alpha = (1 + \epsilon)$ is the solubility fractionation factor (^3He is less soluble) $\simeq 0.988$ (*31*), Δ_4 is the concentration anomaly or percentage supersaturation of ^4He, and all delta values are percentages. Although Δ_3 is therefore a function of both δ_3 and Δ_4, we show in Fig. 7 that Δ_3 is a linear function of δ_3 and thus can be estimated accurately from this parameter alone. The Δ_3 values plotted in Fig. 6 are therefore the "smoothed" values calculated from the least-squares correlation of the Δ_3 and δ_3 data; this reduces the scatter introduced by errors in Δ_4 measurements and also provides Δ_3 values at depths where Δ_4 was not measured. (The actual measured data are, however, plotted in Fig. 7.)
25. We assume that oceanic helium contains two "excess" components: "air injection" helium and "mantle injection" helium, added in varying proportions to the general reservoir of helium at solubility equilibrium with the atmosphere. Air injection helium comes from downward mixing and solution of air bubbles in high latitudes where deep and bottom water form [H. Craig and R. F. Weiss, *Earth Planet. Sci. Lett.* **10**, 289 (1971)]. If this helium has the isotope ratio of air helium (R_{ATM}) and mantle injection helium has a uniform $^3He/^4He$ ratio (R), then in the three-component mixture the anomalies are related by

$$\alpha\Delta_3 = (\delta_3 - \epsilon)(1 + 10^{-2}\,\Delta^\circ_4)/J + \Delta^\circ_4$$

where

$$J = 1 - (1 + 10^{-2}\,\delta_3)/(R/R_{ATM})$$

and Δ°_4 is the ^4He solubility anomaly due to air injection (excluding the mantle injection contribution). This equation is clearly nonlinear for constant R and Δ°_4. To calculate Δ_3 versus δ_3 as a function of R, the air injection anomaly for ^4He has to be determined from the neon concentration anomaly versus solubility (which is entirely due to air injection). The isotope dilution determinations (*10*) show that in this area neon is uniformly supersaturated by 3.5 percent below a depth of 1 km; above 1 km Δ_{Ne} decreases linearly from 3.5 percent to a surface value of 1.5 percent. The corresponding Δ°_4 values ($= 1.28\ \Delta_{Ne}$ from atmospheric and solubility ratios) are 4.5 percent below 1 km and 2 percent in surface water, as observed. We then calculate Δ_3 for the δ_3 profile, taking Δ°_4 as a linear function of depth (and thus of δ_3) from 0 to 1 km, and as a constant 4.5 percent below 1 km, for given values of R. The results for $R/R_{ATM} = 7$, 8, and 9 are shown in Fig. 7. The fact that the relation is linear for $R = 8\,R_{ATM}$ is due to chance: the decrease of Δ°_4 from 1 km to the surface straightens out what is otherwise a curve at $\delta(^3He) < 15$ percent, and happens to match the slope of the relation for depths > 1 km.
26. H. Craig, J. A. Welhan, K. Kim, R. Poreda, J. E. Lupton, *Eos* **61**, 992 (1980).
27. J. A. Welhan and H. Craig, *Geophys. Res. Lett.* **6**, 829 (1979); J. A. Welhan, *Eos* **61**, 996 (1980).
28. G. Klinkhammer, M. Bender, R. F. Weiss, *Nature (London)* **269**, 319 (1977).
29. R. F. Weiss, *Earth Planet. Sci. Lett.* **37**, 257 (1977).
30. Surface tritium values were assumed to be ~ 2.3 tritium units for the South Tow samples; based on the available data [K. L. Michel and H. E. Suess, *Geophys. Res. Lett.* **30**, 4139 (1975); R. A. Fine and H. G. Ostlund, *ibid.* **4**, 461 (1977)]. One tritium unit = $10^{18} \times$ mole fraction ($^3H/^1H$). Thus the surface $\delta(^3He)$ values were adjusted downward by 2.0 percent to correct for the decay of tritium during sample storage.
31. R. F. Weiss, *Science* **168**, 247 (1970).

32. R. Anderson, chief scientist on South Tow leg 8, contributed significantly to this study. One of us (J.E.L.) especially thanks J. Rohrhirsch of the Ministeria de Marina, Lima, for help with the hydrographic work at sea. We also thank F. Dixon, J. Rogers, S. Barker, and K. Craig for assistance with the shipboard collections and analytical work, A. Birket and E. Hernandez for help in the laboratory, and Y. Chung and J. Reid for useful discussions of the hydrographic data. This research was supported by grants from the National Science Foundation and the Office of Naval Research.